Acoustic polarization singularities arising under torsion and orbital angular momentum exchange at the backward collinear acousto-optic diffraction: a case of crystals with point symmetry 3m

Mys O., Kostyrko M., Adamenko D., Skab I. and Vlokh R.

O. G. Vlokh Institute of Physical Optics, 23 Dragomanov Street, 79005 Lviv, Ukraine; vlokh@ifo.lviv.ua

Received: 17.03.2022

Abstract. We consider acousto-elastic effect induced by torsion stresses in $LiNbO_3$ crystals. It is shown that mechanical torsion can give rise to acoustic singularity of the eigenvectors of Christoffel tensor and a torsion-induced 'acoustic birefringence' is conically distributed in space, with an elliptical cross section. This results in appearance of a singly charged acoustic vortex beam that propagates inside the crystal. It is also shown that a backward collinear acousto-optic (AO) interaction of a linearly polarized incident optical wave with a torsion-induced acoustic vortex wave is accompanied by a transfer of orbital angular momentum from the acoustic wave to the diffracted optical wave. If the torsion-induced circular optical vortex wave interacts with the acoustic vortex wave of the same chirality, the diffracted optical wave would bear a doubly charged vortex. In the case of AO interaction of the waves with the opposite chiralities, which bear the vortices having the opposite signs of their charges, the vortices annihilate in the process of AO diffraction and the diffracted optical wave becomes vortex-free.

Keywords: polarization singularities, acoustic waves, orbital angular momentum, collinear acousto-optic diffraction

UDC: 535.42+534.2

1. Introduction

Acousto-optic (AO) diffraction is one of fundamental optical phenomena. It consists in diffraction of optical radiation by the spatial grating of refractive index, which is caused by the strains produced by acoustic wave (AW) via elasto-optic effect (see, e.g., Ref. [1]). The AO diffraction is usually analyzed for the simplest cases when the waves have flat wavefronts. However, the wavefronts of both the optical waves and the AWs can be distorted, which would result in changing directions of their propagation. Moreover, the wavefronts can contain singularities (or screw dislocations) leading to appearance of optical or acoustic vortices [2].

Up to now, the properties of optical vortices and the methods used for their generation are well understood. In particular, it is known that the orbital angular momentum (OAM) carried by a beam with embedded screw dislocation is a quantum value, which equals to $\pm l\hbar$, with $\hbar$ being the reduced Planck's constant and l an integer number called as a topological charge of vortex. The methods of spiral phase plates [3], computer-synthesized holograms [4], q-plates [5] and torsion (or bending) of crystals [6, 7] are among the techniques which are often used for generating the optical vortices. Note that the methods of spiral phase plate and computer-synthesized holograms produce singularities of a scalar field, whereas the q-plates and the inhomogeneous mechanical fields applied to crystals result in polarization (or vector-field) singularities.

In general, the acoustic vortices can be produced in a qualitatively similar manner, although the methods used for their generation have not yet been developed to the extent typical for their

optical counterparts. One can mention at least an opto-acoustic generation method [8], which relies on the light absorption in a spiral phase plate generating AWs, a method of diffraction by an Archimedes spiral [9], and a method of acoustic-vortex generation based on ferroelectret films deposited onto helical surfaces [10]. It is worthwhile that the acoustic vortices can be applied in the same areas as the optical ones. Moreover, the acoustic vortices can be used for implementing levitation [11] and controlling propagation of cracks [12]. It is interesting that the techniques suitable for generating acoustic-polarization singularities have not yet been developed. Perhaps, the reason is that transverse AWs cannot propagate in gaseous or liquid material media, so that the polarization singularities can be induced solely in solid-state media. In other words, the acoustic beam with an embedded polarization singularity must become extinct upon leaving the output surface of a solid-state medium. On the other hand, the acoustic-polarization singularity which is able to generate the acoustic vortex can transfer the OAM to optical beams. This can be implemented in the course of AO diffraction occurring in any solid-state medium and, moreover, the optical beams bearing the OAMs can propagate even in the free space.

To the best of our knowledge, there have been only a few works in the field concerned with AO interactions of vortex beams. These are theoretical consideration of the AO diffraction of Bessel optical beams by the same acoustic beams [13], a study of AO diffraction in optical fibres under conditions of collinear interaction of the optical and acoustic beams bearing vortices [14], experimental demonstration of the fact that the intensity profile and the phase structure of vortex beams are preserved during AO Bragg diffraction [15], experimental finding of an array of optical vortices with fractional charges under the conditions of AO Bragg diffraction [16], a theoretical study of collinear AO diffraction of the circularly polarized optical waves by the circularly polarized AWs in the presence of acoustic conical refraction and optical activity effects [17], and an analysis of backward collinear AO interactions of optical and acoustic vector beams in the centrosymmetric crystals of cubic symmetry where a summing rule for the polarization orders of interacting beams has been formulated [18].

Continuing to develop the above field, in the present work we analyze generation of polarization singularities in the AWs propagating in crystals and study AO interactions of the acoustic and optical waves with polarization singularities.

2. Method of analysis

As an example, we concentrate on $LiNbO_3$ crystals belonging to the point symmetry group 3m [19]. These crystals have their acoustic axes parallel to the three-fold symmetry axis (i.e., the principal axis Z). The quasi-transverse AWs QT_1 and QT_2 with the orthogonal polarizations propagate along this axis with the same velocities (3574 m/s [20]). The elastic-stiffness coefficients of lithium niobate written in matrix notation have earlier been determined under conditions of constant electric field [20]: $C_{11} = 203.0$, $C_{12} = 57.3$, $C_{13} = 75.2$, $C_{33} = 242.4$, $C_{14} = 8.5$, $C_{44} = 59.5$ and $C_{66} = 72.8$ GPa. We consider application of torsion stresses to a cylindrical crystalline rod with the radius 3 mm.

It is known that the AW velocities are coupled with the elastic-stiffness modules via the Christoffel equation:

$$C_{ijkl} m_j m_k p_l = \rho v^2 p_i , \tag{1}$$

where C_{ijkl} is the elastic-stiffness tensor in tensor notation, $\rho = 4640$ kg / m^3 the material density [20], m_j and m_k are the unit wavevectors of the AWs, and p_l and p_i the unit vectors of AW

polarizations. In Eq. (1), the quantity

$$N_{il} = C_{ijkl} m_j m_k \tag{2}$$

represents a second-rank Christoffel tensor. It is symmetric as long as the AW absorption and the acoustic activity are neglected in dielectric media.

The change in the elastic-stiffness coefficients (or the AW velocities) occurring under mechanical stress (or strain) is known as an acousto-elastic effect [21]. It is described by the relation

$$\Delta C_{ijkl} = \theta_{ijklmn} e_{mn} = \theta_{ijklmn} S_{nmrt} \sigma_{rt} = \Theta_{ijklrt} \sigma_{rt}\,, \tag{3}$$

where ΔC_{ijkl} denotes the increment of elastic stiffnesses, θ_{ijklmn} and Θ_{ijklmn} are the sixth-rank polar tensors with the internal symmetry $[[V^2]^2][V^2]$, e_{mn} and σ_{rt} imply respectively the strain and stress tensors, and S_{nmrt} is the tensor of elastic compliances. The acousto-elastic effect is analogical to elasto-optic (or piezo-optic) effect in optics. Note that the changes in the AW velocities induced by the stresses 10^7 N/m^2 are usually small enough (e.g., a few m/s [11]).

The numerical values of the Θ_{ijklrt} components for $LiNbO_3$ are not available in the literature. In our simulations, we have taken the θ_{ijklmn} values which follow from the assumption that the coefficients C_{ijkl} and θ_{ijklmn} have the same order of magnitude [22]. As a result, we have obtained $\Theta_{444} = 0.01$, $\Theta_{344} = 0.03$, $\Theta_{114} = 0.08$, $\Theta_{244} = 0.02$, $\Theta_{144} = 0.04$, $\Theta_{124} = 0.06$ and $\Theta_{134} = 0.07$.

Finally, the acousto-elastic tensor for the symmetry group 3m has been taken from Ref. [23]:

	σ_1	σ_2	σ_3	σ_4	σ_5	σ_6
ΔC_{11}	Θ_{111}	Θ_{112}	Θ_{113}	Θ_{114}	0	0
ΔC_{12}	Θ_{121}	$\Theta_{111}+\Theta_{121}-\Theta_{222}$	Θ_{123}	Θ_{124}	0	0
ΔC_{13}	Θ_{131}	Θ_{132}	Θ_{133}	Θ_{134}	0	0
ΔC_{14}	Θ_{141}	Θ_{142}	Θ_{143}	Θ_{144}	0	0
ΔC_{15}	0	0	0	0	Θ_{244}	$0.5(\Theta_{141}+2\Theta_{241}+\Theta_{142})$
ΔC_{16}	0	0	0	0	$0.5(\Theta_{114}+3\Theta_{124})$	$-0.25(2\Theta_{111}+\Theta_{112}-3\Theta_{222})$
ΔC_{22}	$\Theta_{111}+\Theta_{112}-\Theta_{222}$	Θ_{222}	Θ_{113}	$-\Theta_{114}-2\Theta_{124}$	0	0
ΔC_{23}	Θ_{132}	Θ_{131}	Θ_{133}	$-\Theta_{134}$	0	0
ΔC_{24}	Θ_{241}	$-\Theta_{141}-\Theta_{241}-\Theta_{142}$	$-\Theta_{143}$	Θ_{244}	0	0
ΔC_{25}	0	0	0	0	Θ_{144}	$0.5(\Theta_{141}-\Theta_{142})$
ΔC_{26}	0	0	0	0	$0.5(\Theta_{114}-\Theta_{124})$	$0.25(2\Theta_{111}-\Theta_{112}-\Theta_{222})$

,

	σ_1	σ_2	σ_3	σ_4	σ_5	σ_6
ΔC_{33}	Θ_{331}	Θ_{331}	Θ_{333}	0	0	0
ΔC_{34}	Θ_{341}	$-\Theta_{341}$	0	Θ_{344}	0	0
ΔC_{35}	0	0	0	0	Θ_{344}	Θ_{341}
ΔC_{36}	0	0	0	0	Θ_{134}	$0.5(\Theta_{131}-\Theta_{231})$
ΔC_{44}	Θ_{441}	Θ_{442}	Θ_{443}	Θ_{444}	0	0
ΔC_{45}	0	0	0	0	$-\Theta_{444}$	$-0.5(\Theta_{441}-\Theta_{442})$
ΔC_{46}	0	0	0	0	$0.5(\Theta_{244}-\Theta_{144})$	$0.5(\Theta_{241}+\Theta_{142})$
ΔC_{55}	Θ_{442}	Θ_{441}	Θ_{443}	$-\Theta_{444}$	0	0
ΔC_{56}	$0.5(\Theta_{141}+\Theta_{241}+2\Theta_{142})$	$0.5(\Theta_{141}-\Theta_{241})$	Θ_{143}	$0.5(\Theta_{244}-\Theta_{144})$	0	0
ΔC_{66}	$-0.25\begin{pmatrix}2\Theta_{111}+2\Theta_{121}\\-\Theta_{112}-3\Theta_{222}\end{pmatrix}$	$0.25\begin{pmatrix}2\Theta_{111}-2\Theta_{121}\\+\Theta_{112}-\Theta_{222}\end{pmatrix}$	$0.5(\Theta_{113}-\Theta_{123})$	Θ_{124}	0	0

. (4)

3. Results and discussion

Fig. 1 displays the coordinate dependence of the torsion-induced difference of velocities derived for the transverse AWs. The coordinate dependence of Δv corresponds to a cone under condition of constant torsion moment. This cone is elliptical. The stress-tensor components depend on the torsion moment according to the relation

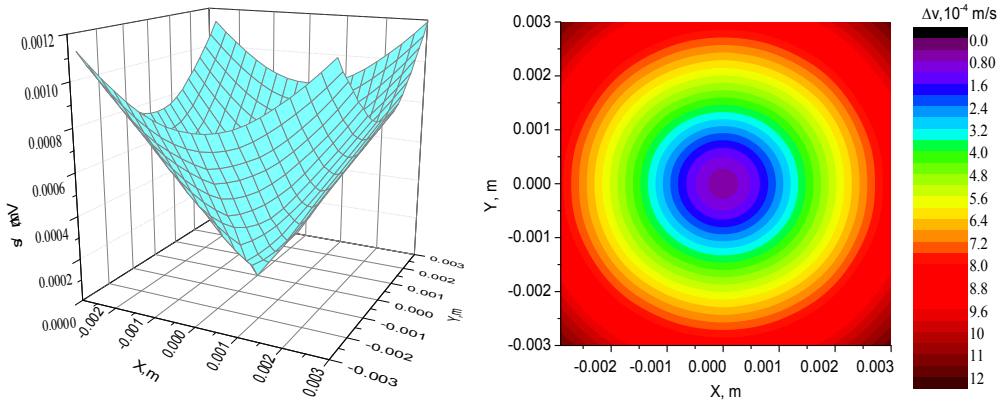

Fig. 1. Conical coordinate dependence of a torsion-induced difference of transverse AW velocities (a) and projection of this dependence in the *XY* plane (b). The torsion moment is equal to M_Z = 0.06 N×m.

$$\sigma_\mu = \frac{2M_z}{\pi R^4}(X\delta_{4\mu} - Y\delta_{5\mu}), \tag{5}$$

where $M_z = \int_S R \times PdS$ stands for the torsion moment, $\delta_{\nu\mu}$ the Kronecker delta, R the radius of crystalline cylinder, S the area of the cylinder base, and P the mechanical load. Therefore, we have two nonzero shear components of the stress tensor, $\sigma_4 = 2\sigma_{32}$ and $\sigma_5 = 2\sigma_{31}$:

$$\sigma_4 = \frac{2M_z}{\pi R^4}X, \tag{6}$$

$$\sigma_5 = \frac{2M_z}{\pi R^4}Y. \tag{7}$$

In other terms, the changes in the AW velocities occurring in the *XZ* and *YZ* planes are induced respectively by the stress components σ_5 and σ_4.

The relations for the components of the Cristoffel tensor are as follows:

$$\begin{aligned} &N_{11} = C_{44} - \Theta_{444}\sigma_4, N_{22} = C_{44} + \Theta_{444}\sigma_4, N_{33} = C_{33}, \\ &N_{23} = \Theta_{344}\sigma_4, N_{13} = \Theta_{344}\sigma_5, N_{12} = -\Theta_{444}\sigma_5. \end{aligned} \tag{8}$$

It is worthwhile that the changes in these components are different for the *XZ* ($\sigma_5 = 0$) and *YZ* ($\sigma_4 = 0$) planes. This leads to different 'acoustic birefringences' induced in these planes. Hence, the influence of torsion moment on the acoustic properties differs from that taking place in crystal optics, where the distribution of induced optical birefringence represents a cone with a circular cross section [6].

The rotation of the eigenvectors of Christoffel tensor around the *Z* axis is given by

$$\tan 2\zeta_Z = \frac{2N_{12}}{N_{11} - N_{22}} = \frac{\sigma_5}{\sigma_4} = \frac{Y}{X} = \tan\varphi, \ \zeta_Z = \frac{1}{2}\varphi, \tag{9}$$

where φ is the polar coordinate ($X = \rho\cos\varphi$ and $Y = \rho\sin\varphi$). Therefore the rotation of the eigenvectors of Christoffel tensor around the *Z* axis is two times smaller than the tracing angle φ. In fact, the torsion of crystal around the *Z* axis produces a topological defect of orientation of the eigenvector of Christoffel tensor, with the defect strength equal to q = ½. In our further analysis,

we will not consider the acoustic conical refraction since along the Z axis the torsion-induced acoustic anisotropy appears.

Let a right-handed circular Gaussian acoustic beam with a small divergence be excited in lithium niobate and propagate along the Z axis. The corresponding displacement vector reads as

$$u^{RH} = u_0 \begin{bmatrix} 1 \\ i \end{bmatrix} e^{i(\Omega t - K_{ac} Z)}, \tag{10}$$

where Ω is the frequency and K_{ac} the wavevector of AW, and u_0 denotes the unit amplitude of displacement vector. [Note that the right-handed polarization is accepted for the case of clockwise rotation of the displacement vector, provided that the observation direction is opposite to K_{ac} – see Ref. [24] where a similar case has been considered in optics]. This wave manifests the spin angular momentum equal to $\hbar$.

When the torsion moment is applied around the Z axis, the 'acoustic birefringence' and the topological defect of the eigenvectors of Christoffel tensor with the strength $q = ½$ appear. Then the initial right-handed circularly polarized Gaussian acoustic beam can be decomposed into the right-handed Gaussian beam and the left-handed beam which bears the acoustic vortex with the charge $l = 2q = 1$. This process can be described in the same way as it has been done in crystal optics [25]:

$$\begin{aligned} u^{out}(\rho,\varphi) = u_0 \cos\frac{\Delta\Gamma_{ac}(\rho, M_z)}{2} \begin{bmatrix} 1 \\ i \end{bmatrix} e^{i(\Omega t - K_{ac} Z)} \\ + i u_0 \sin\frac{\Delta\Gamma_{ac}(\rho, M_z)}{2} \begin{bmatrix} 1 \\ -i \end{bmatrix} e^{i(2q\varphi + 2\zeta_Z^0) + i(\Omega t - K_{ac} Z)} \end{aligned}. \tag{11}$$

Here $\Delta\Gamma_{ac}(\rho, M_z) = \left(\frac{\Omega}{v_{13}(\rho, M_z)} - \frac{\Omega}{v_{23}(\rho, M_z)} \right) d$ is the phase difference between the transverse AWs with the orthogonal polarizations parallel to the X and Y axes, which propagate with the velocities $v_{13}(\rho, M_z)$ and $v_{23}(\rho, M_z)$, d implies the crystal thickness, ζ_Z^0 the angle of orientation of the eigenvectors of Christoffel tensor at $\varphi = 0$ (in our case $\zeta_Z^0 = 0$), and $u^{out}(\rho, \varphi)$ denotes the output-wave amplitude. Eq. (11) describes a conversion of spin angular momentum to OAM, since the second term in the r. h. s. of Eq. (11) describes the AW with a helicoidal phase front, a left-handed polarization, the spin angular momentum equal to $-\hbar$ and the OAM equal to $\hbar$.

Now let us consider a particular case of backward collinear AO diffraction (see Fig. 2). Here the linearly polarized incident optical wave with its polarization parallel to the X (or Y) axis diffracts by the AW bearing the acoustic vortex. Thus following Eq. (11) the displacement vector of AW, which bears vortex can be described by the following relation:

$$u^{LH} = u_0 \sin\frac{\Delta\Gamma_{ac}(\rho, M_z)}{2} \begin{bmatrix} 1 \\ -i \end{bmatrix} e^{i(2q\varphi + 2\zeta_Z^0) + i(\Omega t - K_{ac} Z)}. \tag{12}$$

The strain-tensor components caused by this AW can be represented as

$$\begin{aligned} e_4 = 2e_{23} = \left(\frac{\partial u_2}{\partial Z} + \frac{\partial u_3}{\partial Y} \right) = -K_{ac} e_0 \sin\frac{\Delta\Gamma_{ac}(\rho, M_z)}{2} e^{i2q\varphi + i(\Omega t - K_{ac} Z)}, \\ e_5 = 2e_{13} = \left(\frac{\partial u_1}{\partial Z} + \frac{\partial u_3}{\partial X} \right) = -iK_{ac} e_0 \sin\frac{\Delta\Gamma_{ac}(\rho, M_z)}{2} e^{i2q\varphi + i(\Omega t - K_{ac} Z)}, \end{aligned} \tag{13}$$

with e_0 being the unit strain. Then the electric field components of the diffracted wave can be written as:

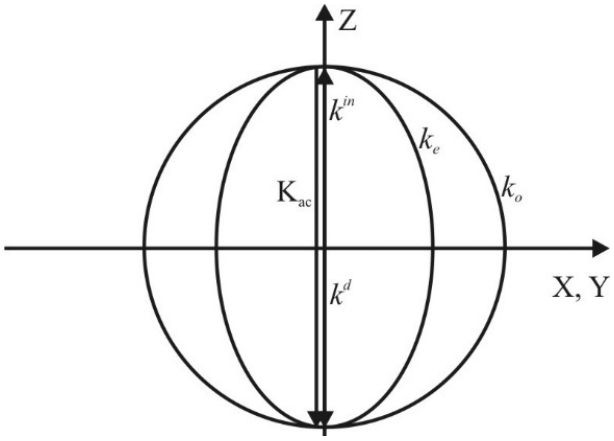

Fig. 2. A schematic view of phase-matching condition provided at backward collinear diffraction: k^{in} and k^d are the wavevectors of incident and diffractive optical waves, and k_o and k_e denote the wavevectors of ordinary and extraordinary optical waves.

$$E_1^d = \Delta B_{11} D_1^{in} = p_{14} e_4 D_1^{in}, \tag{14}$$

or

$$E_2^d = \Delta B_{22} D_2^{in} = -p_{14} e_4 D_2^{in}, \tag{15}$$

where $D_1^{in} = D_0 e^{i(\omega t + k^{in} Z)}$ and $D_2^{in} = D_0 e^{i(\omega t + k^{in} Z)}$ are the electrical inductions of the incident optical waves with the unit amplitude D_0, which are polarized respectively parallel to the X and Y axes, p_{14} is the elasto-optic coefficient, ω the frequency of the incident optical wave, and t the time coordinate. Eqs. (14) and (15) can be rewritten as

$$E_1^d = \Delta B_{11} D_1^{in} = -p_{14} K_{ac} \sin \frac{\Delta\Gamma_{ac}(\rho, M_z)}{2} e^{i([\omega+\Omega]t - [k^{in} - K_{ac}Z]) + i2q\varphi}, \tag{16}$$

or

$$E_2^d = \Delta B_{22} D_2^{in} = p_{14} K_{ac} \sin \frac{\Delta\Gamma_{ac}(\rho, M_z)}{2} e^{i([\omega+\Omega]t - [k^{in} - K_{ac}Z]) + i2q\varphi}. \tag{17}$$

It is evident that the electric field of the diffracted optical wave involves the factor $e^{i2q\varphi}$. Hence, the diffracted beam contains a vortex with the charge $l = 2q = 1$ and, moreover, the OAM is being transferred from the AW to the diffracted optical wave.

Now let us consider the backward collinear AO interaction with the circularly polarized incident optical wave having the right-handed polarization:

$$D^{RH} = D_0 \begin{bmatrix} 1 \\ i \end{bmatrix} e^{i(\omega t + k^{in} Z)}. \tag{18}$$

The electrical induction at the output plane of the crystal can be described by the relation, which consists of the sum of two terms:

$$\begin{aligned} D(\rho, \varphi) = D_0 \cos \frac{\Delta\Gamma_{op}(\rho, M_z)}{2} \begin{bmatrix} 1 \\ i \end{bmatrix} e^{i(\omega t + k^{in} Z)} \\ + iD_0 \sin \frac{\Delta\Gamma_{op}(\rho, M_z)}{2} \begin{bmatrix} 1 \\ -i \end{bmatrix} e^{2iq\varphi + i(\omega t + k^{in} Z)} \end{aligned}, \tag{19}$$

where $\Delta\Gamma_{op}(\rho, M_z) = 2\pi\Delta n(\rho, M_z) d / \lambda$ is the optical phase difference, $\Delta n(\rho, M_z)$ the torsion-

induced optical birefringence, and λ the wavelength of optical radiation. The first term in the r. h. s. of Eq. (19) describes the wave which remains the same as the incident one. On the contrary, the corresponding second term represents the left-handed circular wave bearing a singly charged vortex.

The electric field of the diffracted wave consists of two components:

$$\begin{aligned} E_1^d &= \Delta B_{11} D_1^{in} + \Delta B_{12} D_2^{in} \\ &= -i2 p_{14} K_{ac} \sin\frac{\Delta\Gamma(\rho, M_z)}{2} \sin\frac{\Delta\Gamma_{op}(\rho, M_z)}{2} e^{i4q\varphi + i(\omega+\Omega)t + (k^{in} - K_{ac})Z}, \end{aligned} \tag{20}$$

$$\begin{aligned} E_2^d &= \Delta B_{22} D_2^{in} + \Delta B_{21} D_1^{in} \\ &= 2 p_{14} K_{ac} \sin\frac{\Delta\Gamma(\rho, M_z)}{2} \sin\frac{\Delta\Gamma_{op}(\rho, M_z)}{2} e^{i4q\varphi + i(\Omega+\omega)t + (k^{in} - K_{ac})Z}. \end{aligned} \tag{21}$$

The resulting electric field of the diffracted wave is given by

$$\begin{aligned} E^d &= \sqrt{(E_1^d)^2 + (E_2^d)^2} \\ &= 2 p_{14} K_{ac} \sin\frac{\Delta\Gamma(\rho, M_z)}{2} \sin\frac{\Delta\Gamma_{op}(\rho, M_z)}{2} e^{i4q\varphi + i(\Omega+\omega)t + (k^{in} - K_{ac})Z}. \end{aligned} \tag{22}$$

As seen from Eq. (22), the diffracted wave bears a doubly charged vortex with the charge equal to $2\hbar$. In other words, the charges of the vortices referred to the acoustic and optical waves are being summed up. It is also obvious that the signs of charges of the vortices carried by the interacting acoustic and optical waves are opposite whenever these waves have the opposite chiralities. Then the appropriate vortices must annihilate and the diffracted wave becomes vortex-free.

Of course, the acoustic vortex beam cannot be separated from the acoustic Gaussian wave beam inside the crystal, and the same is true of the optical beams. In this case, the AO interaction occurs between the 'mixed' waves, so that the diffracted optical vortex wave will be mixed, too. However, the diffracted optical vortex beam can be separated from the Gaussian beam by a circular polarizer.

Finally, let us notice that the effects described above can exist in the crystals that belong to the symmetry groups 3m, 32, $\bar{3}$m, 3, $\bar{3}$, 23, m3, 432, $\bar{4}$3m and m3m, provided that the torsion moment is applied along the three-fold symmetry axis.

3. Conclusion

In the present work, we have considered the acousto-elastic effect induced by mechanical torsion stresses in the canonical $LiNbO_3$ crystal. We have demonstrated that the torsion stresses can impose the acoustic singularity of the eigenvectors of Christoffel tensor. In addition, the 'acoustic birefringence' induced by the torsion is characterized by the conical spatial distribution, of which cross section is elliptical. This results in arising of a singly charged acoustic vortex beam that propagates inside the crystal.

We have also shown that the process of backward collinear AO interaction of the linearly polarized incident optical wave with the torsion-induced acoustic vortex wave is accompanied by a transfer of OAM from the AW to the diffracted optical wave. If the torsion-induced circular optical vortex wave interacts with the acoustic vortex wave of the same chirality, the diffracted optical wave bears a doubly charged vortex. In the case of AO interaction of the waves with the opposite chiralities and the vortices with the opposite signs of charges, the latter vortices annihilate in the process of AO diffraction so that the diffracted optical wave becomes vortex-free.

References

1. Magdich L N and Molchanov V Ya. Acoustooptic devices and their applications. New York: Gordon and Breach Science Publisher, 1989.
2. Nye J F and Berry M V, 1974. Dislocations in wave trains. Proc. Roy. Soc. A. **336**: 165–190.
3. Beijersbergen M W, Coerwinkel R P C, Kristensen M and Woerdman J P, 1994. Helical-wavefront laser beams produced with a spiral phaseplate. Opt. Commun. **112**: 321–327.
4. Basistiy V, Bazhenov Yu, Soskin M S and Vasnetsov M V, 1993. Optics of light beams with screw dislocations. Opt. Commun. **103**: 422–428.
5. Marrucci L, Manzo C and Paparo D, 2006. Optical spin-to-orbital angular momentum conversion in inhomogeneous anisotropic media. Phys. Rev. Lett. **96**: 163905.
6. Skab I, Vasylkiv Y, Savaryn V and Vlokh R, 2011. Optical anisotropy induced by torsion stresses in $LiNbO_3$ crystals: appearance of an optical vortex. J. Opt. Soc. Amer. A. **28**: 633–640.
7. Skab I, Vasylkiv Y and Vlokh R, 2012. Induction of optical vortex in the crystals subjected to bending stresses. Appl. Opt. **51**: 5797–5805.
8. Gspan S, Meyer A, Bernet S and Ritsch-Marte M, 2004. Optoacoustic generation of a helicoidal ultrasonic beam. J. Acoust. Soc. Amer. **115**: 1142–1146.
9. Jimenez N, Pico R, Sanchez-Morcillo V, Romero-Garcia V, Garcia-Raffi L M and Staliunas K, 2016. Formation of high-order acoustic Bessel beams by spiral diffraction gratings. Phys. Rev. E. **94**: 053004.
10. Ealo J, Prieto J and Seco F, 2011. Airborne ultrasonic vortex generation using flexible ferroelectrets. IEEE Trans. Ultrason. Ferroel. Freq. Control. **58**: 1651–1657.
11. Hong Z Y, Yin J F, Zhai W, Yan N, Wang W L, Zhang J and Drinkwater B W, 2017. Dynamics of levitated objects in acoustic vortex fields. Sci. Rep. **7**: 7093.
12. Psakhie S G, Shilko E V, Popov M V and Popov V L, 2015. Key role of elastic vortices in the initiation of intersonic shear cracks. Phys. Rev. E. **91**: 063302.
13. Belyi V N, Khilo P A, Kazak N S and Khilo N A, 2016. Transformation of phase dislocations under acousto-optic interaction of optical and acoustical Bessel beams. J. Opt. **18**: 074002.
14. Dashti P Z, Alhassen F and Lee H P, 2006. Observation of orbital angular momentum transfer between acoustic and optical vortices in optical fiber. Phys. Rev. Lett. **96**: 043604.
15. Martynyuk-Lototska I, Vasylkiv Y, Dudok T, Skab I and Vlokh R, 2018. Acoustooptic operation of optical vortex beams. Optik. **155**: 179–184.
16. Vasylkiv Y, Martynyuk-Lototska I, Skab I and Vlokh R, 2018. Generation of an optical vortex array in the course of acousto-optic diffraction. Appl. Opt. **57**: 10284–10289.
17. Kostyrko M, Skab I and Vlokh R, 2021. Angular-momentum exchange among acoustic and optical waves at the collinear acousto-optic diffraction. J. Opt. **23**: 064003.
18. Kostyrko M, Vasylkiv Y, Skab I and Vlokh R, 2021. Collinear acousto-optic interaction of optical and acoustic vector beams. Summation of the polarization orders of topological defects. Optik. **244**: 167552.
19. Shaskolskaya M P. Acoustic crystals. Moscow: Nauka, 1982.
20. Smith R T and Welsh F S, 1971. Temperature dependence of the elastic, piezoelectric, and dielectric constants of lithium tantalate and lithium niobate. J. Appl. Phys. **42**: 2219–2230.
21. Huang Xiaojun, Burns D R and Toksoz M N, 2001. The effect of stresses on the sound velocity in rocks: Theory of acoustoelasticity and experimental measurements. Massachusetts Institute of Technology. Earth Resources Laboratory. http://hdl.handle.net/1721.1/68599.
22. Hmiel A, Winey J M, Gupta Y M and Desjarlais M P, 2016. Nonlinear elastic response of

strong solids: First-principles calculations of the third-order elastic constants of diamond. Phys. Rev. B. **93**: 174113.
23. Vedam K and Srinivasan R, 1967. Non-linear piezo-optics. Acta Cryst. **22**: 630–634.
24. Azzam R M A and Bashara N M. Ellipsometry and polarized light. Amsterdam, New York: North-Holland, 1977.
25. Marrucci L, 2008. Generation of helical modes of light by spin-to-orbital angular momentum conversion in inhomogeneous liquid crystals. Mol. Cryst. Liq. Cryst. **48**: 148–162.

Mys O., Kostyrko M., Adamenko D., Skab I. and Vlokh R. 2022. Acoustic polarization singularities arising under torsion and orbital angular momentum exchange at the backward collinear acousto-optic diffraction: a case of crystals with point symmetry 3m. Ukr.J.Phys.Opt. **23**: 107 – 115. doi: 10.3116/16091833/23/2/107/2022

Анотація. *Розглянуто акустопружний ефект, викликаний торсійними напруженнями в кристалах $LiNbO_3$. Показано, що механічне кручення може спричинити акустичну сингулярність власних векторів тензора Крістофеля, а індуковане крученням «акустичне подвійне променезаломлення» конічно розподілене в просторі, з еліптичним поперечним перерізом. Це приводить до появи однозарядного акустичного вихрового променя, який поширюється всередині кристала. Також показано, що зворотна колінеарна акустооптична (АО) взаємодія лінійно поляризованої падаючої оптичної хвилі з акустичною вихровою хвилею, індукованою крученням, супроводжується передаванням орбітального кутового моменту від акустичної хвилі до дифрагованої оптичної хвилі. Якщо індукована крученням циркулярно поляризована оптична вихрова хвиля взаємодіє з акустичною вихровою хвилею тієї ж хіральності, то дифрагована оптична хвиля буде нести подвійно заряджений вихор. У разі АО-взаємодії хвиль з протилежними хіральностями, які несуть вихори з протилежними знаками заряду, вихори анігілюють в процесі АО-дифракції, а дифрагована оптична хвиля стає безвихровою.*